Supplemental Information

Supplemental Figures

Figure S1

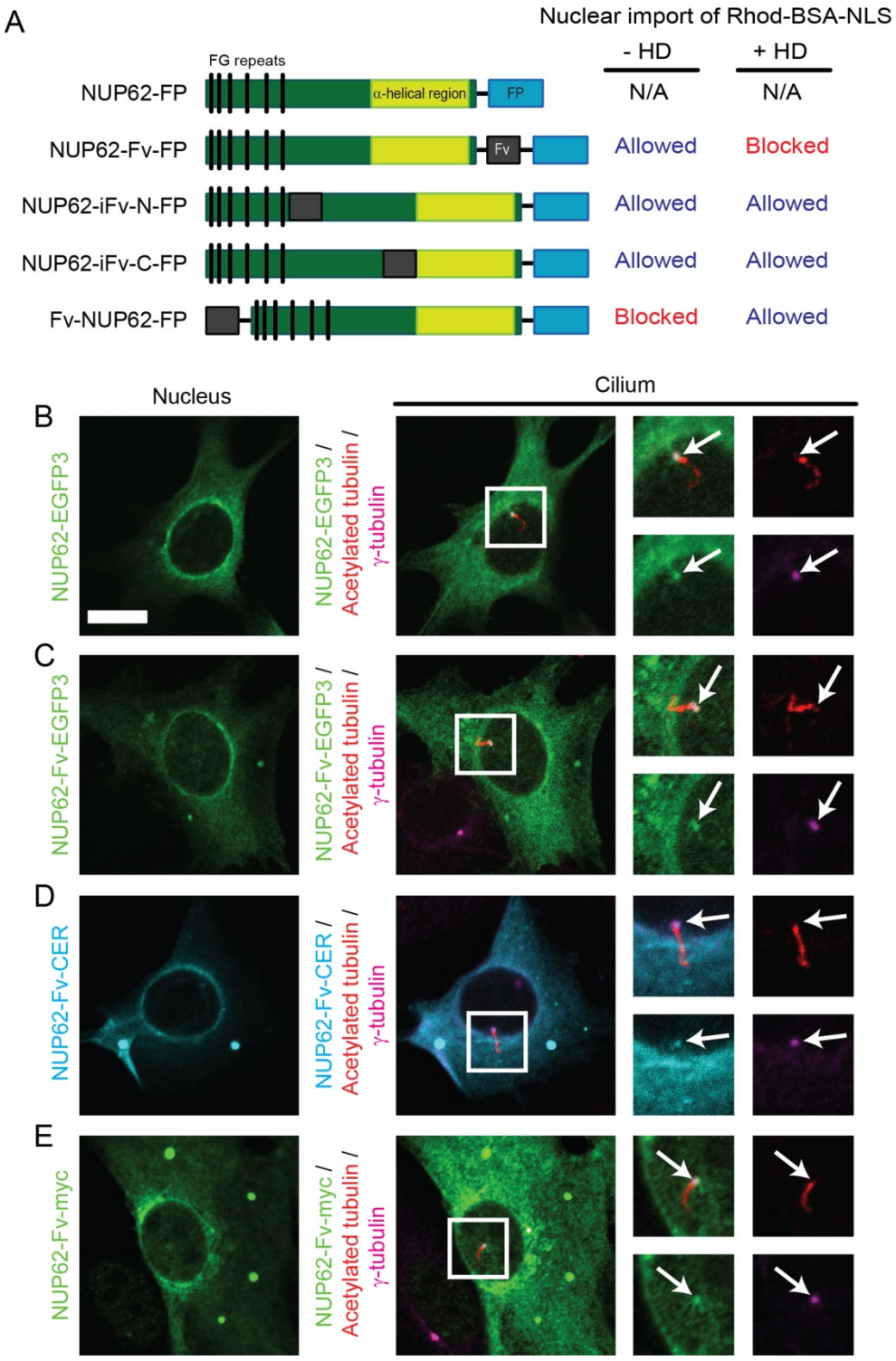

Figure S1. Schematic of NUP62 constructs and their localization in cells. (A) Schematic of NUP62 constructs tagged with Fv domain and EGFP3 (FP). The functional output of each construct was tested in NIH 3T3 cells by microinjecting rhod-BSA-NLS into expressing cells treated with vehicle (-HD) or HD. Fluorescence images were captured over time and the amount of rhod-BSA-NLS in the nuclear compartment was measured after 20 min. Placement of the Fv domain at the C-terminus of NUP62 (NUP62-Fv-EGFP3 construct) allowed rhod-BSA-NLS import into the nucleus in the absence of HD but blocked nuclear import in the presence of HD. Placement of the Fv domain at internal regions of NUP62 (NUP62-iFv-N-EGFP3 and NUP62-iFV-C-EGFP3 constructs) allowed rhod-BSA-NLS import in the absence and presence of HD. Thus, these constructs were not pursued further. Surprisingly, placement of the Fv domain at the N-terminus of NUP62 (Fv-NUP62-EGFP3 construct) blocked rhod-BSA-NLS import into the nucleus in the absence of HD but allowed nuclear import in the presence of HD. The mechanism behind this finding is unclear and this construct was also not pursued further. (B–E) Confocal images of NIH 3T3 cells expressing NUP62-Fv constructs. Images taken at focal planes of the mid-nucleus and the cilium are shown. When expressed in NIH 3T3 cells, NUP62-EGFP3 (B), NUP62-Fv-EGFP3 (C), NUP62-Fv-Cer (D) and NUP62-Fv-myc (E) localize to the nuclear envelope (circular pattern around the nucleus) and the ciliary base (arrows). Thus, ciliary localization of NUP62 is independent of the Fv and FP tags. Magnified images of the ciliary region are shown to the right of each panel. Scale bar, 10 μm.

Figure S2

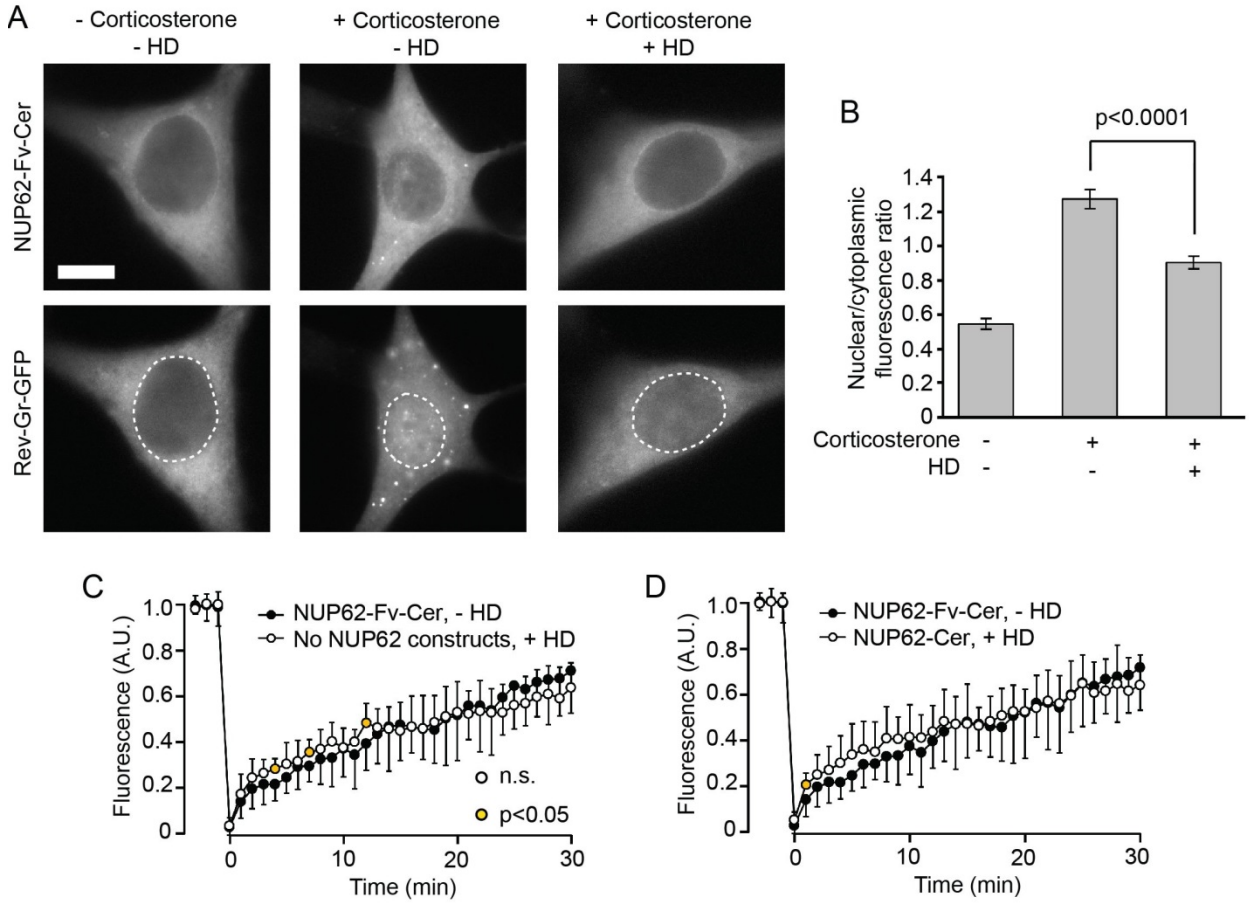

Figure S2. Forced dimerization of NUP62-Fv attenuated active transport of Rev-Gr-GFP into the nucleus and homodimerizer alone does not affect ciliary import of KIF17-mCit. (A,B) Nuclear import of Rev-Gr-GFP. (A) Representative images of NIH 3T3 cells transfected with NUP62-Fv-Cer (top row) and Rev-Gr-GFP (bottom row). Rev-Gr-GFP localized to the cytosol (left panel) but was induced to enter the nuclear compartment upon corticosterone addition (middle panel, 60 min incubation). Nuclear import of Rev-Gr-GFP was attenuated in the presence of HD (right panel). Dashed lines indicate nuclei. Scale bar, 10 μm. (B) Quantification of nuclear import of Rev-Gr-GFP 60 min after stimulation with corticosterone. Data are presented as mean ± SEM. n = 19–21 cells each. (C, D) Effect of HD on ciliary import of KIF17-mCit. FRAP of KIF17-mCit in the presence of HD was determined either in (C) untransfected cells or (D) cell expressing NUP62-Cer (lacking the Fv domain) and is compared to FRAP in the absence of HD (NUP62-Fv-Cer expressing cells from Figure 1G). Addition of HD did not affect FRAP rates of KIF17-mCit in the absence of the Fv domain. Error bars show SD. n = 11 cells each.

Figure S3

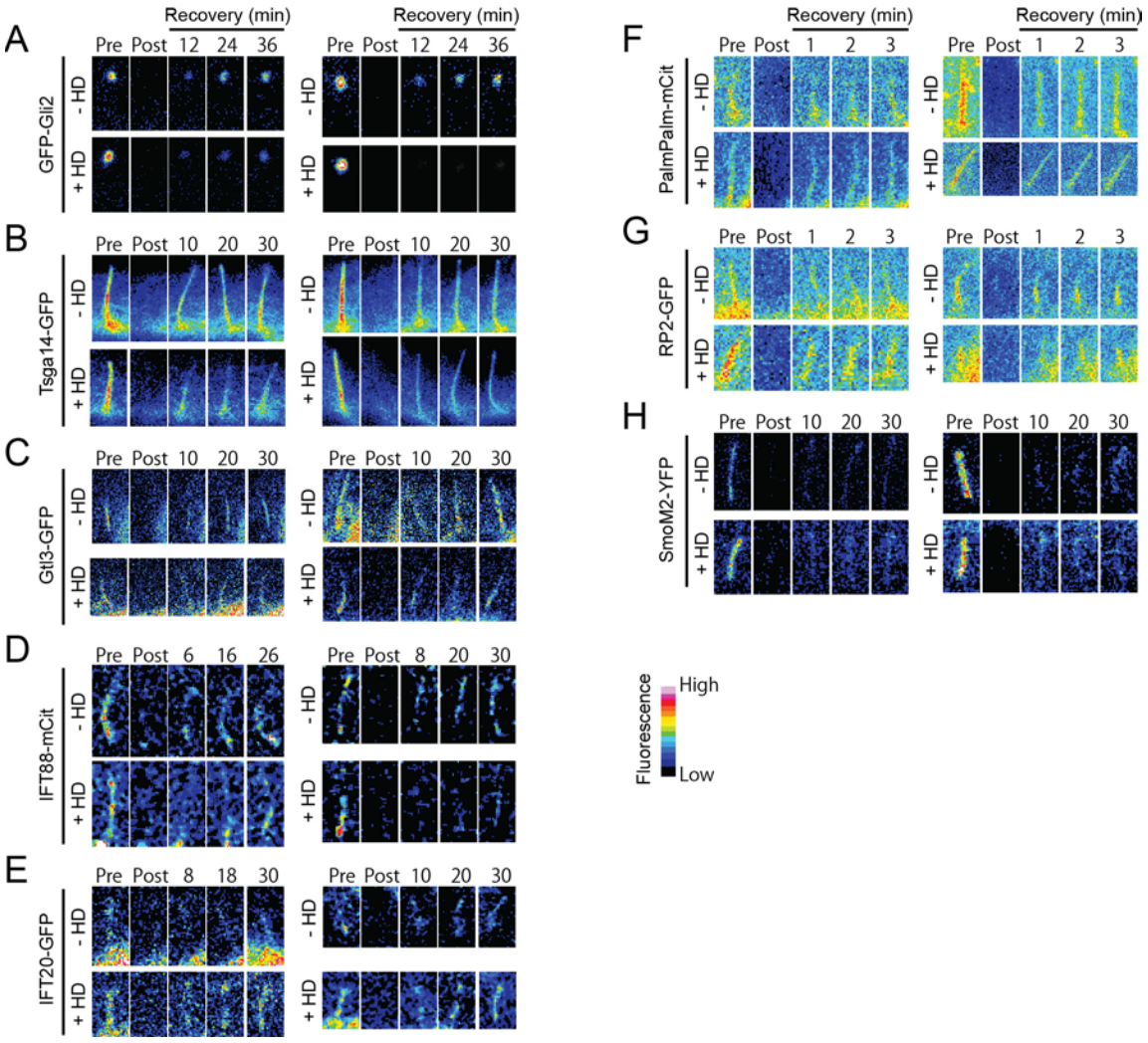

Figure S3. FRAP of ciliary proteins. Representative images taken from FRAP time course of the indicated ciliary proteins. Two example images are shown for each condition. Pseudo-color images are shown and a median filter (radius, 1 pixel) was applied to IFT88-mCit and IFT20-GFP images for viewing purpose. Pre, prebleach; Post, postbleach; and the recovery numbers indicate the time after bleaching (min).

Figure S4

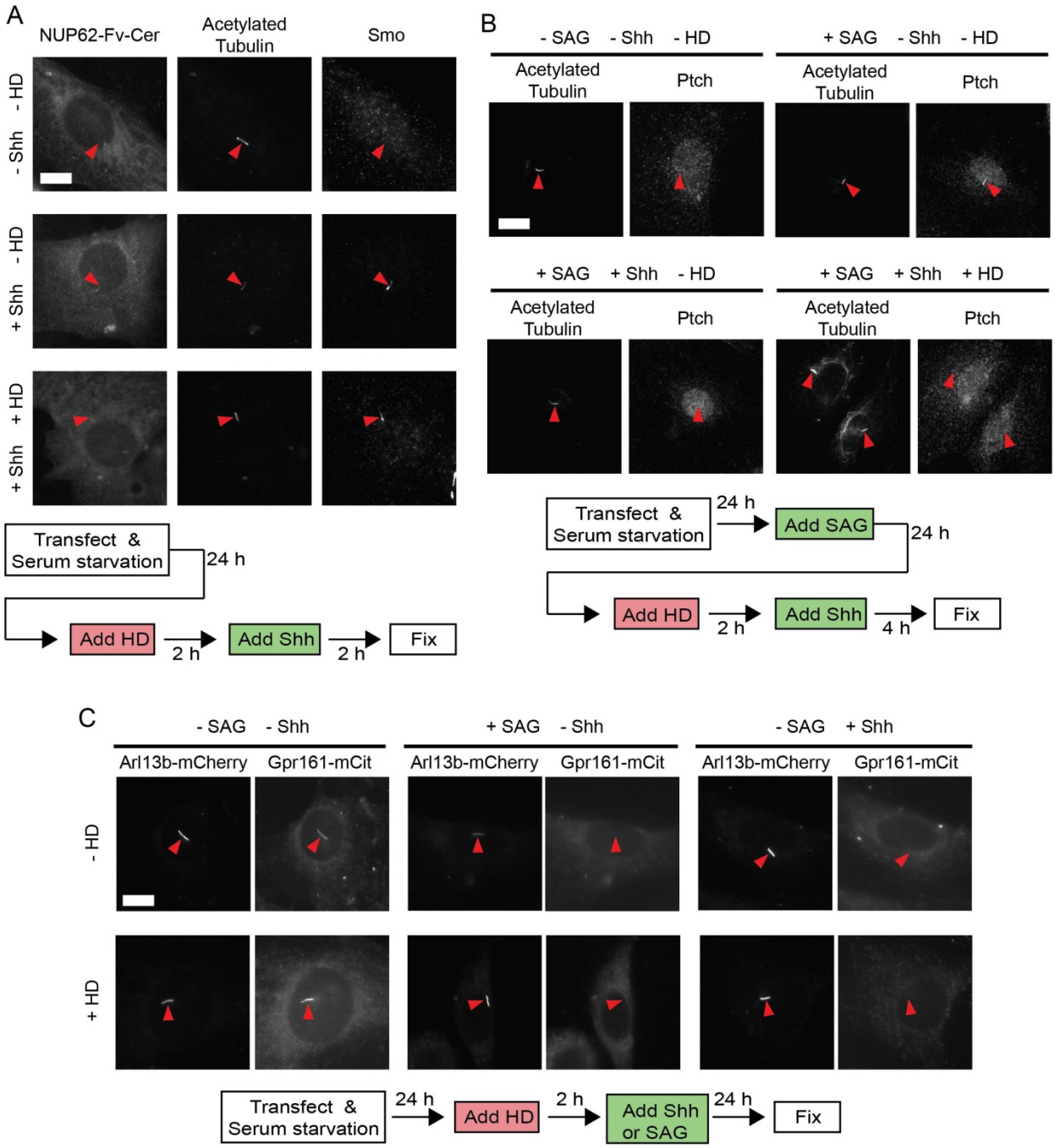

Figure S4. Effect of forced dimerization of NUP62-Fv-Cer on ciliary transport of transmembrane proteins. (A–C) Representative fluorescence images of fixed NIH 3T3 cells used to obtain data in Figure 4D–F, respectively. Arrowheads indicate positions of cilia. Flow diagrams of the experimental procedures for the assays are shown at the bottom of each figure. Scale bar, 10 μm.